Electronic Supplementary Information

Electrocatalytic nitrate reduction to ammonia via amorphous cobalt boride

Yongbin Shi,[a] Suxian Xu[a] and Fei Li*[a]

[a] State Key Laboratory of Fine Chemicals, DUT-KTH Joint Education and Research Centre on Molecular Devices, Dalian University of Technology, Dalian, 116024, China.

E-mail: lifei@dlut.edu.cn

Experimental section

Chemicals

Cobalt (II) chloride hexahydrate ($CoCl_2 \cdot 6H_2O$), Sodium borohydride ($NaBH_4$), Potassium hydroxide (KOH), Sodium citrate dihydrate ($C_6H_5Na_3O_7 \cdot 2H_2O$), Salicylic acid ($C_7H_6O_3$), Sodium hydroxide (NaOH), Ammonium chloride (NH_4Cl), Potassium nitrate-N^{15} ($K^{15}NO_3$), Hydrazine standard solution (analytical standard, 1000 μg mL^{-1}), Sodium nitroprusside dihydrate ($C_5FeN_6Na_2O \cdot 2H_2O$), Sulfanilamide ($C_6H_8N_2O_2S$), N-(1-naphthyl) ethylenediamine dihydrochloride ($C_{12}H_{14}N_2 \cdot 2HCl$), p-Dimethylaminobenzaldehyde ($C_9H_{11}NO$), 1,10-Phenanthroline ($C_{12}H_8N_2$), Ammonium Ferric Sulfate Solution ($FeH_4NO_8S_2$, 5%), and Sodium acetate (CH_3COONa) were purchased from Macklin chemical company and without any further purification. Ethanol, hydrochloric acid, Phosphoric acid, Sulfuric acid, Potassium nitrate (KNO_3), and sodium hypochlorite solution ($\rho Cl \geq 10.0\%$) were analytical pure and obtained from commercial supplier. The carbon paper (CP) was purchased from TORAY Industries, Japan. Millipore water (resistivity: ca. 18 MΩ cm) was applied to prepare the electrolyte solution.

Preparation of CoB$_x$ nanoparticles[1]

The amorphous cobalt boride nanoparticles were synthesized by chemical reduction method. Due to a large amount of hydrogen was generated during the reaction, the entire synthesis process was carried out in a fume hood. In a typical synthesis, 0.2g $CoCl_2 \cdot 6H_2O$ was completely dissolved in 2 mL deionized water to form solution A. 0.3783g $NaBH_4$ was added to 2mL deionized water to form solution B. Both the solution A and B were kept in the ice bath for 20 min. Then solution B was slowly droped into solution A and a lot of bubbles were quickly generated. The reaction lasted for about 60 minutes until there were no bubbles generated. The black precipitate was collected by centrifugation and extensively washed with deionized water and ethanol to remove any traces of unreacted ions. The black powder was obtained by freeze drying overnight and was stored in a glove box to prevent oxidation.

Preparation of metallic Co nanoparticles[2]

The entire synthesis process was carried out in a fume hood. 1.0 g $CoCl_2 \cdot 6H_2O$ was added to 7.5 mL of ethanol. A white slurry prepared by mixing 2.5 g of NaOH with 5 mL of 50% $N_2H_4 \cdot H_2O$ solution was added to the above solution under magnetic stirring. The produced precipitate was washed with a lot of deionized water and ethanol. The grey powder was obtained by freeze drying overnight and was stored in a glove box to prevent oxidation.

Preparation of the working electrodes

5 mg of catalyst and 40 μL of 5 wt.% Nafion solution were dispersed in 960 μL ethanol with ultrasonically for 60 min to form a homogeneous ink. Then, 40 μL of ink was coated on carbon paper (CP, 1×0.5 cm^2), which will be dried at room temperature. The obtained mass loading was 0.4 mg cm^{-2}.

Characterization

X-ray diffraction (XRD) pattern was obtained on D/max-2400 diffractometer (Japan Rigaku Rotaflex) with Cu Kα radiation (λ = 154.1 Å) to obtain the crystal structure. The morphology of as-prepared catalysts was studied by Ultrahigh Resolution Field Emission Scanning Electron Microscopy (FESEM, JSM-7900F) equipped with energy-dispersive X-ray spectroscopy (EDX). The selective area electron diffraction (SAED) and microstructure of the materials were characterized by transmission electron microscopy (TEM, FEI TF 30). The element composition and states of the materials were performed by X-ray photoelectron spectroscopy (XPS) (Thermo Scientific ESCALAB 250). Specially, the binding energy was standardized concerning to the C 1s peak at 284.7 eV. 1H-NMR spectra were collected at 298K using Bruker DRX-600 NMR. UV-Vis absorption spectra were recorded on a UV-Vis spectrophotometer (Shimadazu, UV-1800). Inductively coupled plasma atomic emission spectrometer (ICP-AES) was performed on a PerkinElmer model AVIO 500.

Electrochemical measurements

All electrochemical measurements were conducted on a CHI 660E

electrochemical workstation (Shanghai Chenhua Instrument Co., Ltd) with a three-electrode system at room temperature. The reaction was assessed using a gas-tight, two-compartment cell separated by a Nafion membrane (Nafion 117). In a typical test, the CP depositing with catalyst was used as the working electrode, Hg/HgO as a reference electrode was placed in the cathode chamber, while in the anode, the platinum mesh electrode was severed as the counter electrode. Electrolyte solution (30 mL) was Ar-saturated of 0.1 M KOH with 0.05 M KNO_3 and was evenly distributed to the cathode and anode compartments. Before the experiment, the Nafion membrane was treated in H_2O_2 (5%) aqueous solution at 80 °C for 2 h. Then, the membrane was boiled in 0.5 M H_2SO_4 aqueous solution for 2 h at 80 °C, and subsequently boiled in deionized water for 2 h at 80 °C.

All potentials mentioned in this work was correspond to the reversible hydrogen electrode potential (RHE), where $E_{RHE} = E_{Hg/HgO} + 0.0591pH + E^{\theta}_{Hg/HgO}$. The current densities were normalized to the geometric area of the working electrode unless otherwise stated. The entire electrolysis had sustained for 1 h under a certain potential. The linear sweep voltammetry (LSV) at a scan rate of 5 mV/s.

The turnover frequency (TOF) was calculated using the following formula: TOF= jA / 8nF, where j is the current density at an overpotential of -0.9 V *vs.* RHE, A is the geometric area of the working electrode, 8 is the number of electrons transferred to produce one molecule of ammonia, n is the number of moles of active sites, and F is Faraday constant (96485 C mol^{-1}).[3]

Determination of ion concentration

The indophenols blue method and ammonia-selective electrode analysis were applied to determine the production of ammonia, nitrite was tested by colorimetric method, hydrazine was evaluated by the Watt and Chrisp method, and hydroxylamine was tested by colorimetric method.

Determination of NH_4^+

a) Indophenols blue method[4]

Typically, a certain amount of electrolyte was taken out from the cathode chamber

and diluted to 2 mL with deionized water. The diluted electrolyte mixed with 2 mL 1.0 M NaOH solution containing salicylic acid (5 wt%) and sodium citrate (5 wt%), 1 mL 0.05 M NaClO and 200 μL 1 wt% sodium nitroprusside dihydrate aqueous solution. The mixture was stood for 2 h to ensure complete color development. The absorbance of the mixture was measured with UV-vis absorption spectrum at 655 nm. The concentration-absorbance curve was calibrated using a series of standard ammonium chloride solutions.

b) Ammonia-selective electrode method

20 mL of electrolyte was pipetted from the post-electrolysis electrolyte and mixed with 0.2 mL of Ionic Strength Adjuster (ISA). The measurement was then recorded using an ammonia ion selective electrode (at least 2 minutes are necessary to get stable readings).

Determination of NO_2^-[5]

A mixture of p-aminobenzenesulfonamide (2 g), N-(1-Naphthyl) ethylenediamine dihydrochloride (0.1 g), ultrapure water (25 mL) and phosphoric acid (5 mL, ρ=1.70 g/mL) was used as a color reagent. A certain amount of electrolyte was taken out from the cathode chamber and diluted to 5 mL with deionized water. Next, 0.1 mL color reagent was added into the aforementioned 5 mL solution and mixed uniformity, and the absorption intensity at a wavelength of 540 nm was recorded after sitting for 20 min. The concentration-absorbance curve was calibrated using a series of standard sodium nitrite solutions.

Determination of hydrazine[4]

Briefly, a mixture of 5.99 g of p-$C_9H_{11}NO$, 30 mL of concentrated HCl, and 300 mL of ethanol was applied as a color reagent. 2 mL of post-electrolysis electrolyte and 2 mL of color reagent mixed and stirred for 10 min at room temperature. The resulting solutions were measured with UV-vis absorption spectra at 455 nm.

Determination of hydroxylamine[6]

The quantification of NH_2OH was based on its reduction of Fe^{3+} to Fe^{2+}, the latter forms an orange complex with 1,10-phenanthroline. In detail, 100 μL of an aqueous

acetate buffer (1 M sodium acetate and 1 M acetic acid mixture), 100 µL of a 4 mM ammonium ferric sulfate aqueous solution and 100 µL of a 10 mM 1,10-phenanthroline ethanolic solution were sequentially added into 3mL of the sample. The resulting solutions were measured with UV-Vis absorption spectra on the basis of their maxmum absorbance at 510 nm, and the concentration was quatified by the calibration cuve, which was established using a series of standard samples with known concentratons of hydroxylamine.

Calculations of the NH_3 yield rate, NH_3 Faradaic Efficiency and NO_2^- Faradaic Efficiency of NitRR:

The NH_3 yield rate and faradic efficiency were calculated by the following equations:

$$NH_3\ yield\ rate\ = \frac{C_{NH_3} \times V}{M_{NH_3} \times t \times S}$$

$$FE_{NH_3} = \frac{8F \times C_{NH_3} \times V}{M_{NH_3} \times Q} \times 100\%$$

The NO_2^- faradic efficiency were calculated by the following equations:

$$FE_{NO_2^-} = \frac{2F \times C_{NO_2^-} \times V}{M_{NO_2^-} \times Q} \times 100\%$$

Where C_{NH_3} is the measured average NH_3 mass concentration, V is the volume of the electrolyte (30 mL), M_{NH_3} is the molar mass of NH_3, t is the reaction time (1 h), S is the geometric area of working electrode (0.5 cm^2), F is the Faraday constant (96485 C mol^{-1}), and Q is the total charge passed through the electrode, $C_{NO_2^-}$ is the measured average NO_2^- mass concentration, $M_{NO_2^-}$ is the molar mass of NO_2^-.

^{15}N isotopic experiment

The ^{15}N isotopic labeled experiment was operated to clarify the source of ammonia by using the ^{15}N isotopic (K^{15}NO$_3$, 99.99%). 0.1 M KOH containing 0.05M K^{15}NO$_3$ was used as electrolyte. After electroreduction, 2 mL electrolyte was extracted from the

cathode compartment and the pH value was adjusted to be weak acid with 8 M HCl. Then, 0.6 mL d[6]-DMSO was added to 50 μL the aforementioned mixed solution for further characterization by ^{1}H NMR (600 MHz). The ^{1}H NMR (600 MHz) spectra of electrolyte adopting K^{15}NO$_3$ as reactants showed typical double peaks of ^{15}NH$_4^+$, while the ^{1}H NMR (600 MHz) spectra of electrolyte adopting K^{15}NO$_3$ as reactants showed typical triple peaks of ^{14}NH$_4^+$. This result reveals that the produced ammonium is completely derived from nitrate reduction.
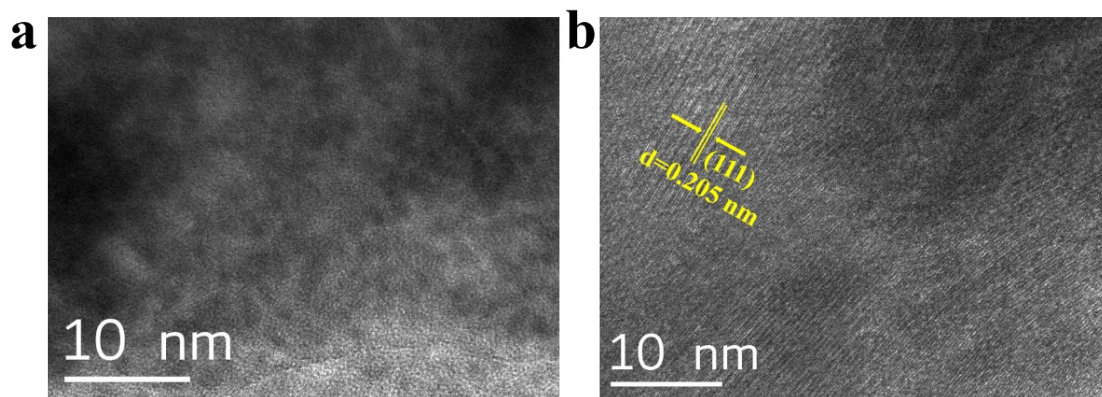
Fig. S1 HR-TEM images of (a) CoB$_x$ and (b) Co nanoparticles.
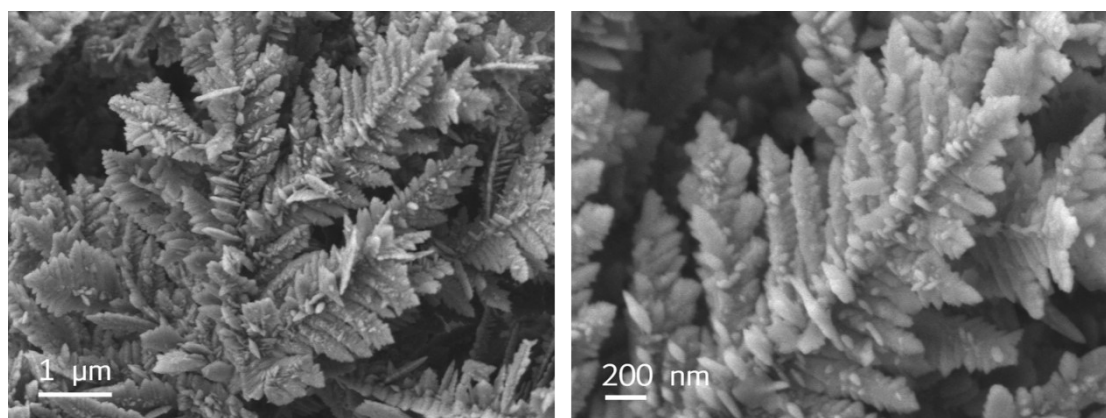
Fig. S2 SEM images of Co.
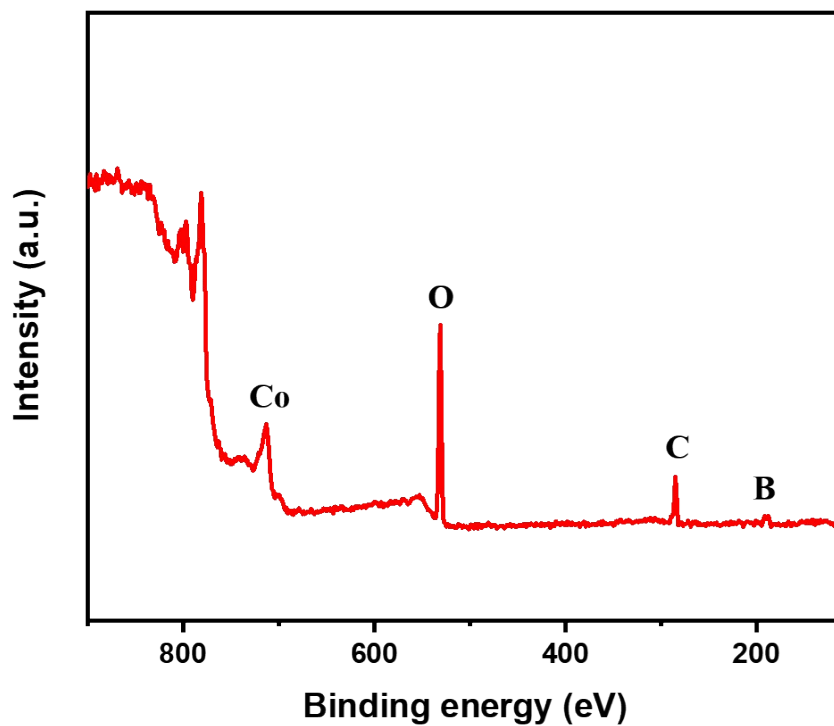
Fig. S3 XPS survey spectra of CoB$_x$.
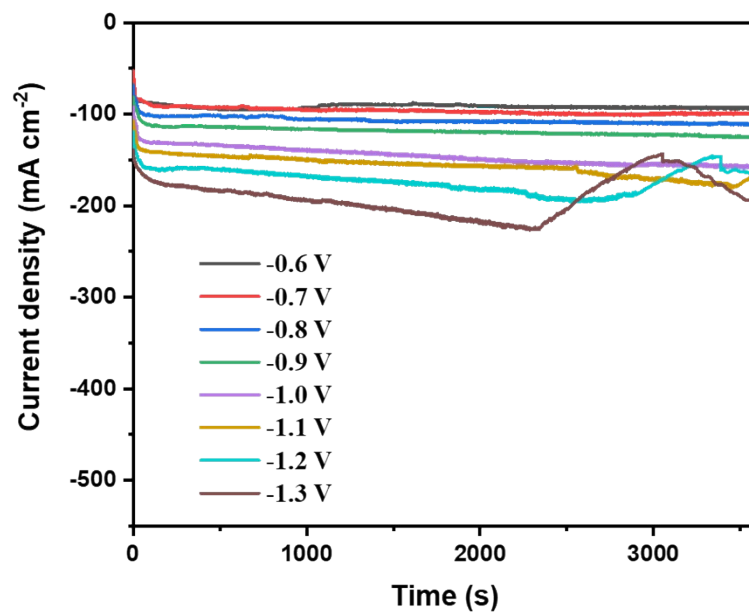
Fig. S4 Chronoamperometric curves of CoB$_x$ at various potentials.
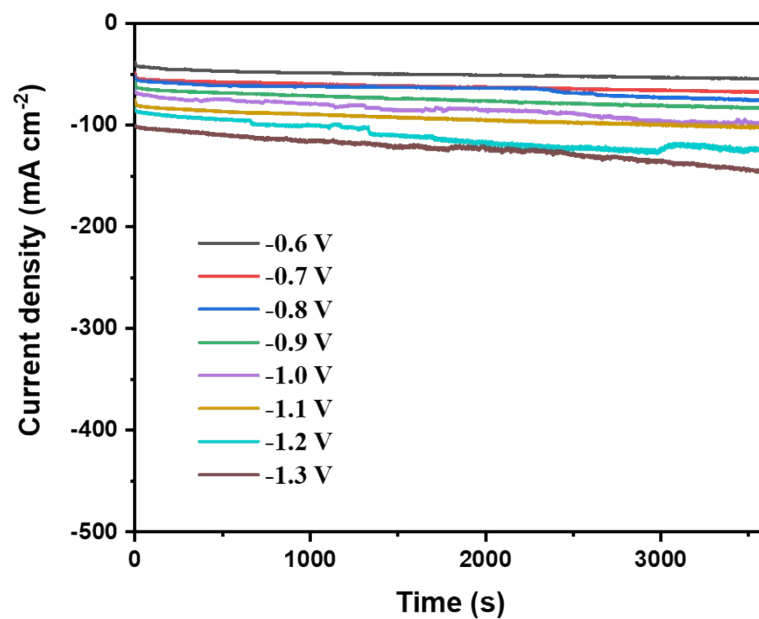
Fig. S5 Chronoamperometric curves of Co at various potentials.
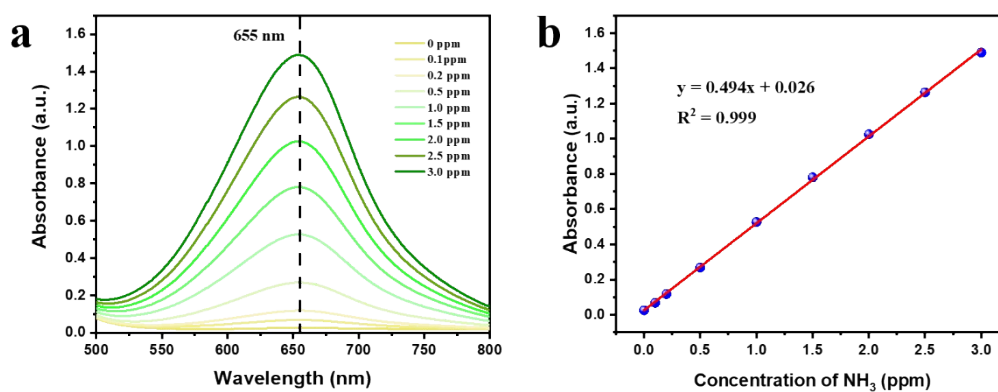
Fig. S6 (a) UV-Vis absorption spectra of various NH_3 concentrations after incubated for 2 h at room temperature. (b) Calibration curve used for calculation of NH_3 concentrations.
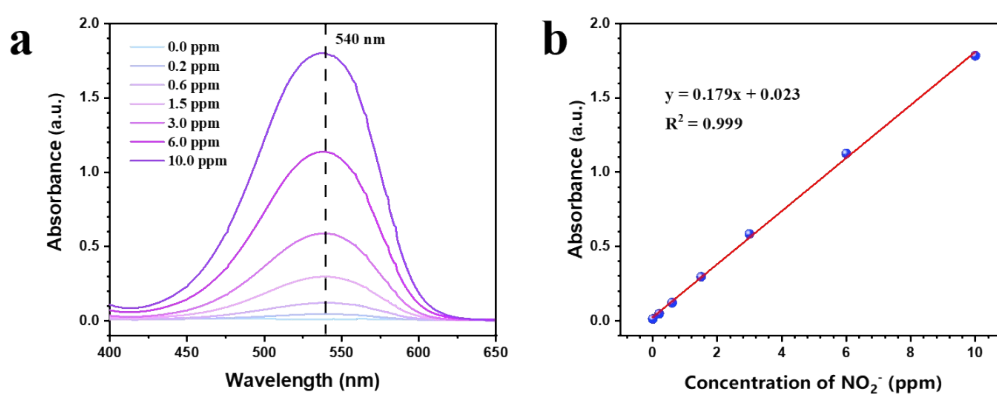
Fig. S7 (a) UV-Vis spectra of various NO_2^- concentrations after incubated for 20 min at room temperature. (b) Calibration curve used for estimating the concentrations of NO_2^-.
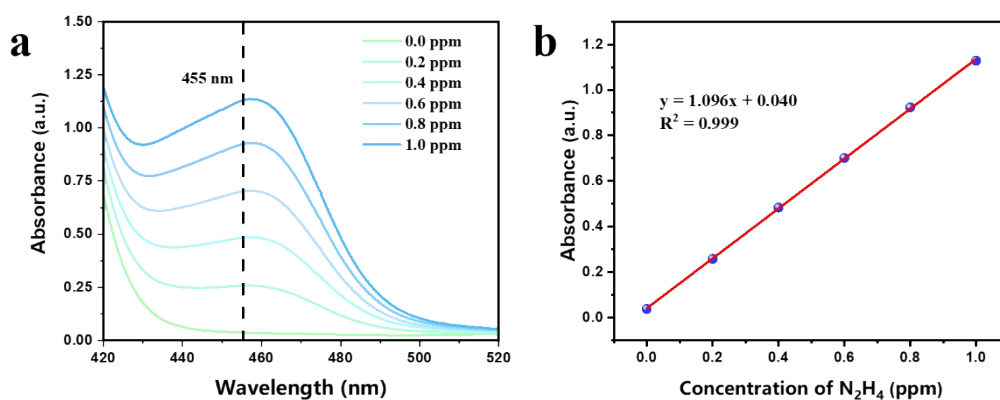
Fig. S8 (a) UV-Vis absorption spectra at various N_2H_4 concentrations after incubated for 10 min at room temperature. (b) Calibration curve used for calculation of N_2H_4 concentrations.
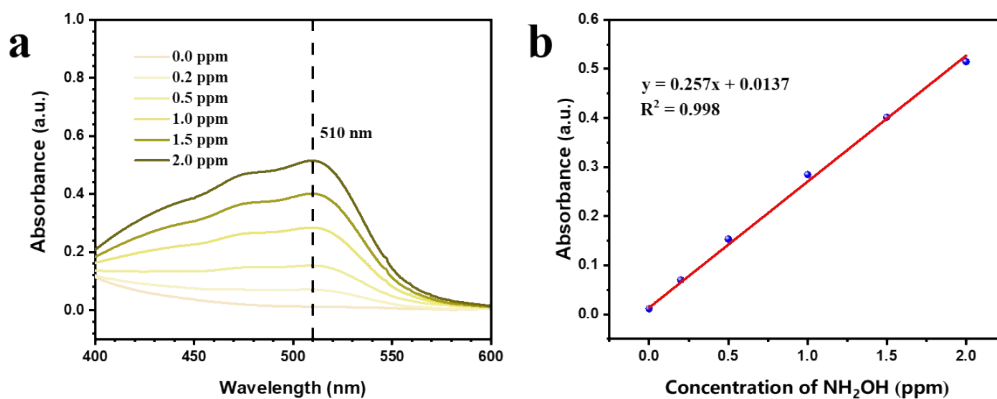
Fig. S9 (a) UV-Vis absorption spectra at various NH_2OH concentrations after incubated for 10 min at room temperature. (b) Calibration curve used for calculation of NH_2OH concentrations.
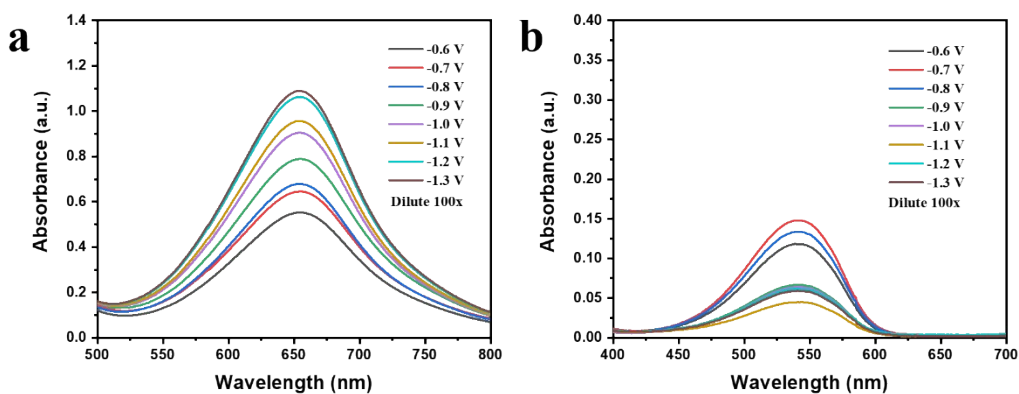
Fig. S10 UV-Vis absorption spectra of the 0.1 M KOH electrolytes with 0.05 M KNO_3 (after electrolysis with CoB_x catalysts at different applied potentials for 1 h) after incubated for (a) 2 h and (b) 20 min at room temperature, respectively.
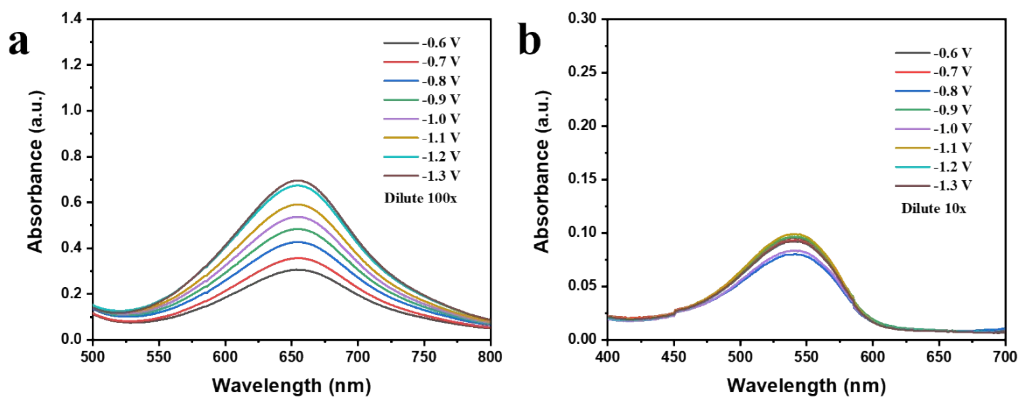
Fig. S11 UV-Vis absorption spectra of the 0.1 M KOH electrolytes with 0.05 M KNO_3 (after electrolysis with Co catalysts at different applied potentials for 1 h) after incubated for (a) 2 h and (b) 20 min at room temperature, respectively.
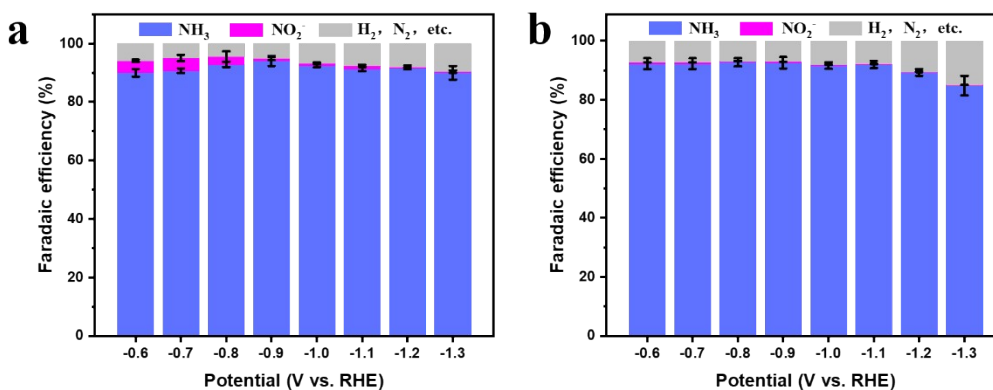
Fig. S12 Selectivity of (a) CoB_x and (b) Co at different given potentials. (Error bars were derived from experimental results of three independent samples)
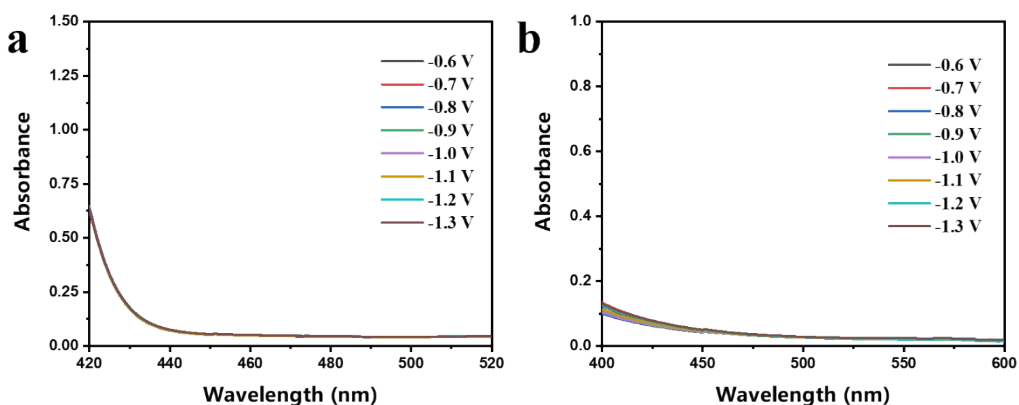
Fig. S13 UV-Vis absorption spectra of the 0.1 M KOH electrolytes with 0.05 M KNO_3

(after electrolysis with CoB$_x$ catalysts at different applied potentials for 1 h) after incubated for 10 min at room temperature.
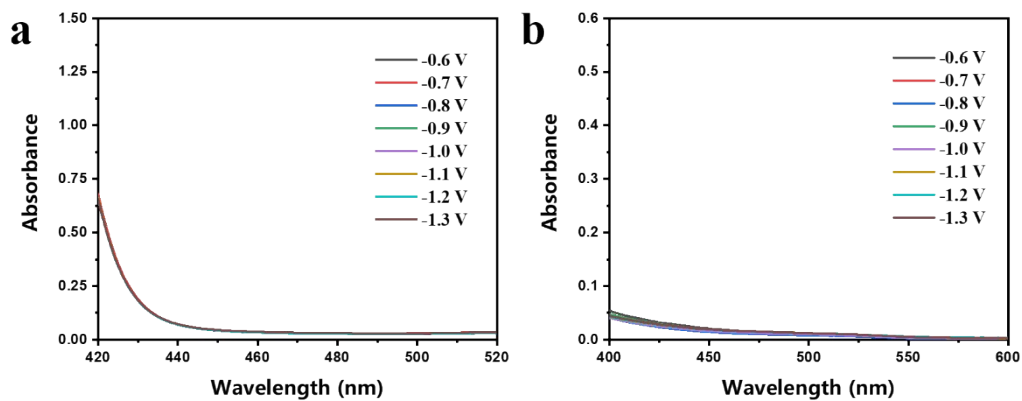
Fig. S14 UV-Vis absorption spectra of the 0.1 M KOH electrolytes with 0.05 M KNO$_3$ (after electrolysis with Co catalysts at different applied potentials for 1 h) after incubated for 10 min at room temperature.
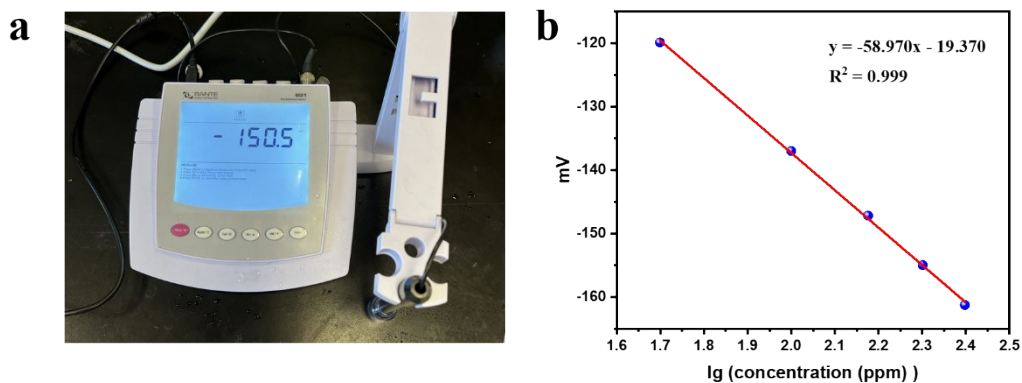
Fig. S15 (a) Photograph of ammonia-sensitive electrode. (b) The standard curve of NH$_4$Cl solution with different concentration detected by ammonia-sensitive electrode.
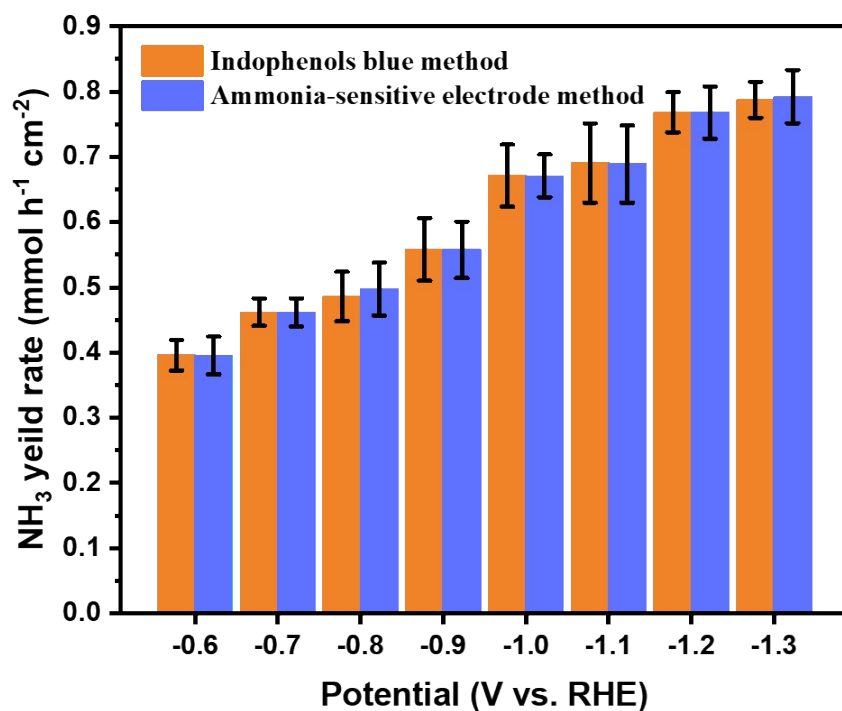
Fig. S16 Comparison of ammonia calibrated by indophenols blue method and ammonia-sensitive electrode method. (Error bars was derived from experimental results from three independent samples)
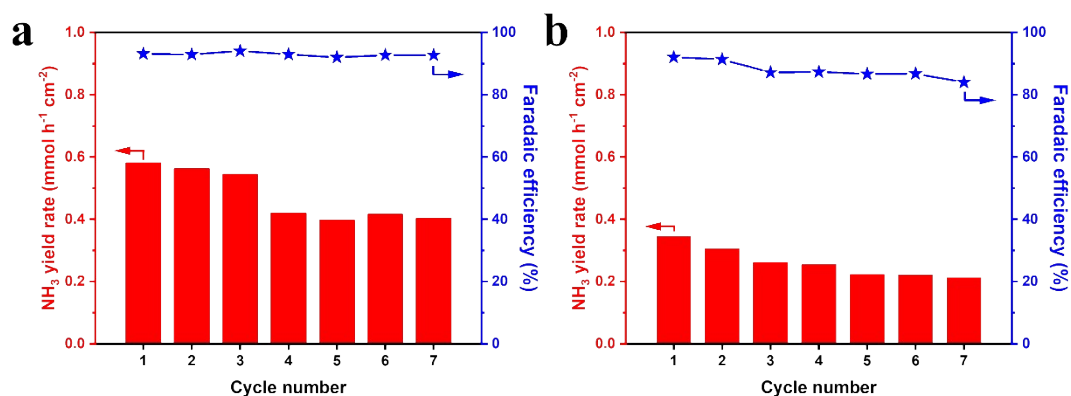
Fig. S17 NH_3 yield rates and FEs of recycling tests over (a) CoB_x and (b) Co at -0.9 V *vs.* RHE in 0.1 M KOH with 0.05 M KNO_3.
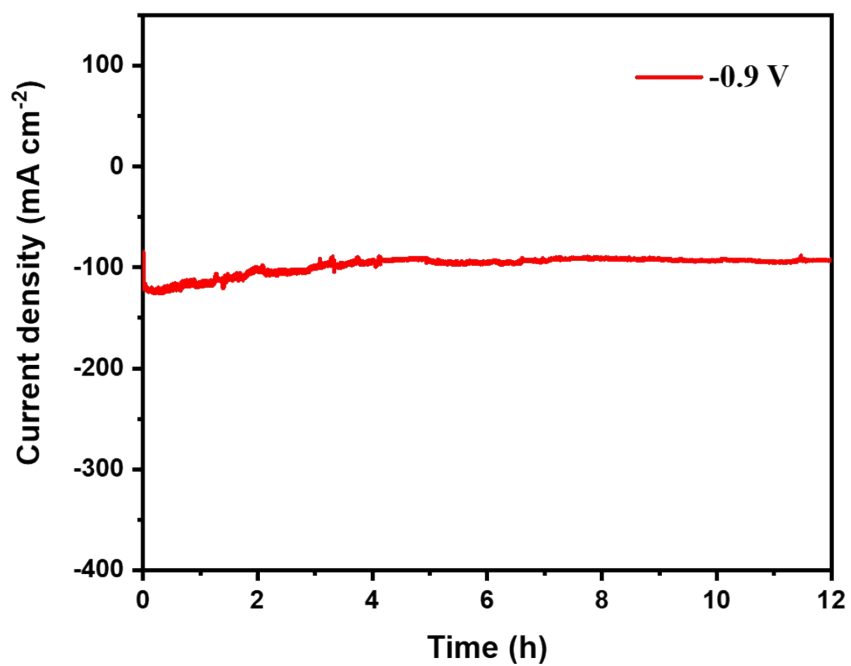
Fig. S18 Chronoamperometric curve of CoB$_x$ for 12 h at -0.9 V *vs.* RHE in 150 mL of 0.1 M KOH with 0.05 M KNO$_3$.
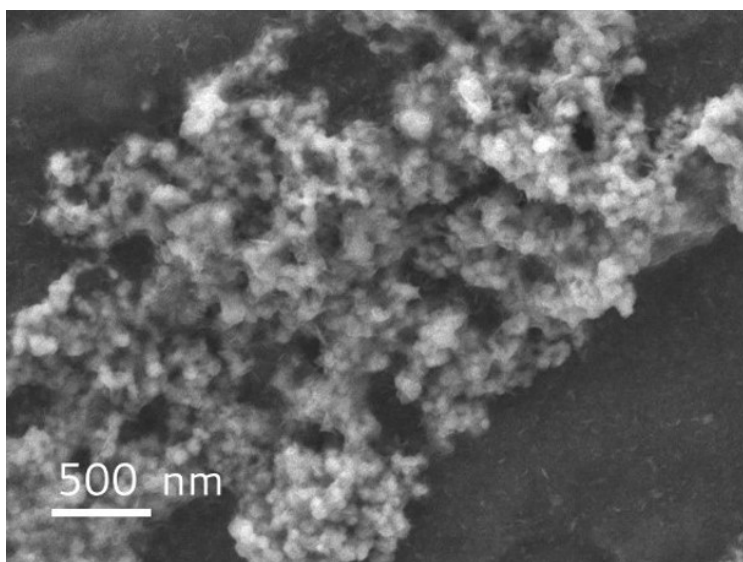
Fig. S19 SEM image of CoB$_x$ after successive cycling electrolysis at the potential of -0.9 *vs.* RHE.
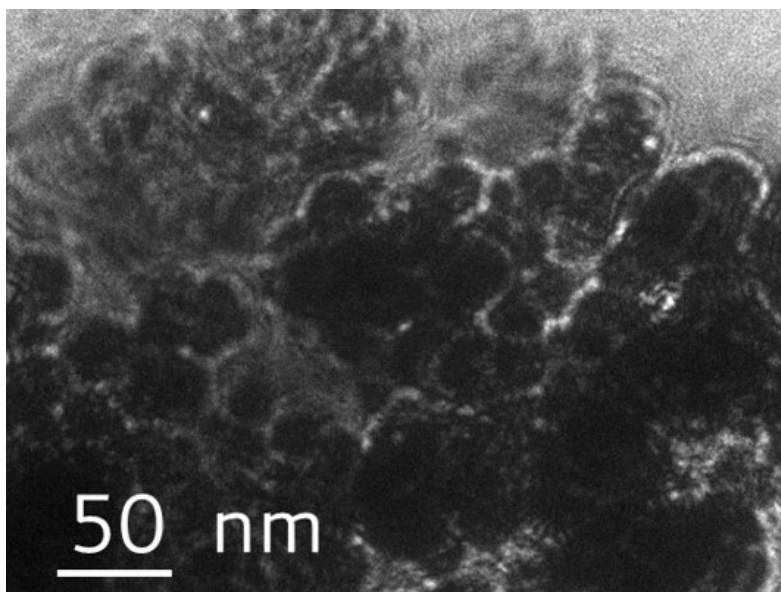
Fig. S20 TEM image of CoB$_x$ after successive cycling electrolysis at a potential of -0.9 *vs.* RHE.
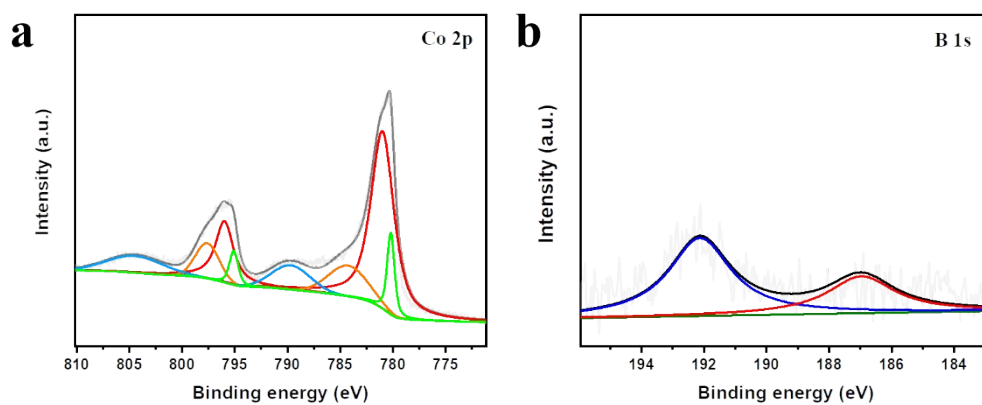
Fig. S21 High-resolution XPS spectra of (a) Co 2p and (b) B 1s of CoB$_x$ after electrolysis at a potential of -0.9 *vs.* RHE.
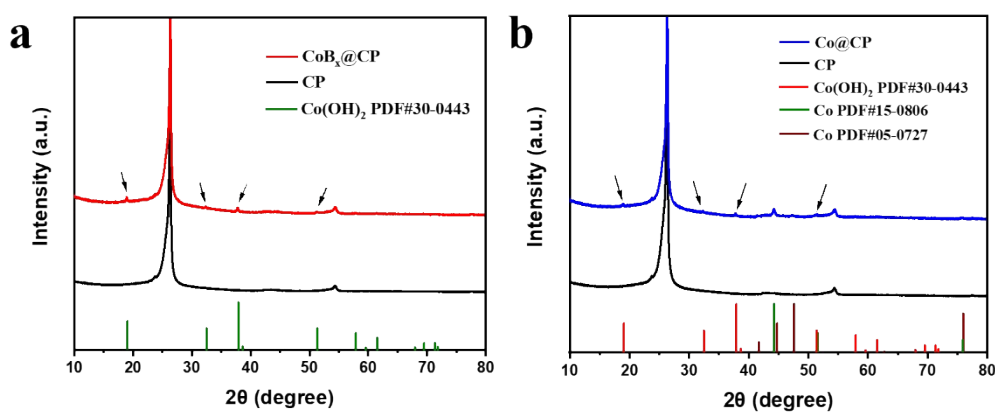
Fig. S22 XRD patterns of (a) CoB_x and (b) Co after electrolysis at a potential of -0.9 *vs.* RHE in 0.1 M KOH with 0.05 M KNO_3.
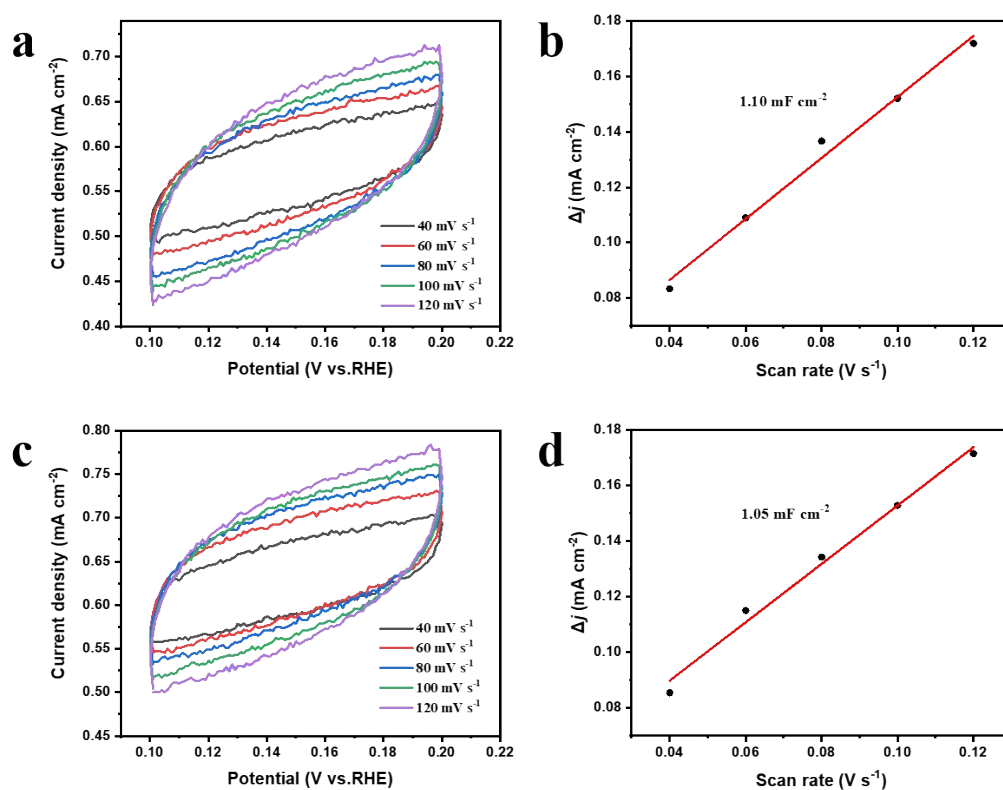
Fig. S23 CV curves of (a) CoB_x, and (c) Co at different scan rates (40, 60, 80, 100, and 120 mV s^{-1}) in the potential range of 0.1-0.2 V *vs.* RHE. (b and d) corresponding current density variation plotted against the scan rate, fitted to a linear regression, enables the estimation of the double-layer capacitance (C_{dl}).
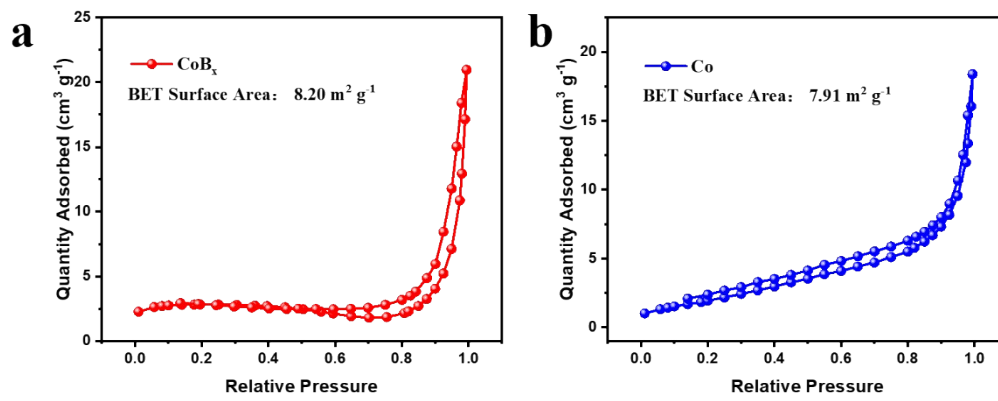
Fig. S24 Nitrogen adsorption-desorption isotherms of (a) CoB_x (b) Co.

Table S1. Elemental compositions of CoB_x nanoparticles quantified by ICP-AES.

Composition (wt. %)	B	Co
	9.95	86.39

Table S2. Atomic concentration of CoB_x nanoparticles from the XPS results.

Atomic (%)	Co	B	O
	19.04	17.93	38.13

Table S3 Comparison of NH_3 yield rate and Faradaic efficiency (NH_3) between CoB_x, and recently-reported electrocatalysts.

Materials	Electrolyte	NH_3 yield rates @ Potential (V vs. RHE)	FE(NH_3) @ Potential (V vs. RHE)	Ref.
CoB_x	0.1 M KOH + 0.05 M NO_3^-	0.558 ± 0.048 mmol h^{-1} cm^{-2} @-0.9 1.395 ± 0.120 mmol h-1 mg_{cat}^{-1} @-0.9 0.787 ± 0.028 mmol h-1 cm-2 @-1.3 1.968 ± 0.069 mmol h-1 mg_{cat}^{-1} @-1.3	94.00 ± 1.67 % @-0.9 89.99 ± 2.33 % @-1.3	This work
PTCDA/O-Cu	0.1 M PBS + 500 ppm NO_3^-	436 ± 85 µg h^{-1} cm^{-2} / 0.0256 ± 0.005 mmol h^{-1} cm^{-2}	77 ± 3 %	2020[7]
Cu/Cu_2O NWAs	0.5 M Na_2SO4 + 200 ppm NO_3^-	0.2447 mmol h^{-1} cm^{-2}	95.8 %	2020[5]
Ir nanotubes	0.1 M $HClO_4$ + 1 M $NaNO_3$	0.0542 mmol h^{-1} mg_{cat}^{-1}	84.7 %	2020[8]
CoP PANSs	0.5 M K_2SO_4 + 0.05 M KNO_3	0.1296 mmol h^{-1} cm^{-2}	94.24 ± 2.8 %	2021[9]
TiO_{2-x}	0.5 M Na_2SO_4 + 50ppm $NaNO_3$	0.045 mmol h^{-1} mg_{cat}^{-1}	85 %	2020[10]
PP-Co/CP	0.1 M NaOH + 0.1 M $NaNO_3$	1.1 mmol h-1 mg_{cat}^{-1}	90.1 %	2022[11]
Fe SAC	0.10 M K_2SO_4 + 0.5 M NO_3^-	0.46 mmol h-1 cm^{-2}	~ 75 %	2021[12]
$Cu_{50}Ni_{50}$ alloy	1 M KOH + 0.1 M KNO_3		~ 99 ± 1 %	2020[13]
$Ni_3B@NiB_{2.74}$	0.1 M KOH + 0.1 M NO_3^-	198.3 µmol h^{-1} cm^{-2}	100 %	2021[2]

References

1. J. F. Gao, J. F. Hou and L. B. Kong, *Part. Part. Syst. Char.* 2021, **38**, 2100020.
2. L. Li, C. Tang, X. Cui, Y. Zheng, X. Wang, H. Xu, S. Zhang, T. Shao, K. Davey and S. Z. Qiao, *Angew. Chem. Int. Ed.*, 2021, **60**, 14131-14137.
3. S. Xie, F. Li, S. Xu, J. Li and W. Zeng, *Chin. J. Catal.*, 2019, **40**, 1205-1211.
4. Z. Fang, P. Wu, Y. Qian and G. Yu, *Angew. Chem. Int. Ed.*, 2021, **60**, 4275-4281.
5. Y. Wang, W. Zhou, R. Jia, Y. Yu and B. Zhang, *Angew. Chem. Int. Ed.*, 2020, **59**, 5350-5354.
6. Y. Wu, Z. Jiang, Z. Lin, Y. Liang and H. Wang, *Nat. Sustainability*, 2021, **4**, 725-730.
7. G.-F. Chen, Y. Yuan, H. Jiang, S.-Y. Ren, L.-X. Ding, L. Ma, T. Wu, J. Lu and H. Wang, *Nat. Energy*, 2020, **5**, 605-613.
8. J. Y. Zhu, Q. Xue, Y. Y. Xue, Y. Ding, F. M. Li, P. Jin, P. Chen and Y. Chen, *ACS Appl. Mater. Interfaces*, 2020, **12**, 14064-14070.
9. Y. Jia, Y. G. Ji, Q. Xue, F. M. Li, G. T. Zhao, P. J. Jin, S. N. Li and Y. Chen, *ACS Appl. Mater. Interfaces*, 2021, **13**, 45521-45527.
10. R. Jia, Y. Wang, C. Wang, Y. Ling, Y. Yu and B. Zhang, *ACS Catal.*, 2020, **10**, 3533-3540.
11. Q. Chen, J. Liang, Q. Liu, K. Dong, L. Yue, P. Wei, Y. Luo, Q. Liu, N. Li, B. Tang, A. A. Alshehri, M. S. Hamdy, Z. Jiang and X. Sun, *Chem. Commun.*, 2022, **58**, 4259-4262.
12. Z. Y. Wu, M. Karamad, X. Yong, Q. Huang, D. A. Cullen, P. Zhu, C. Xia, Q. Xiao, M. Shakouri, F. Y. Chen, J. Y. T. Kim, Y. Xia, K. Heck, Y. Hu, M. S. Wong, Q. Li, I. Gates, S. Siahrostami and H. Wang, *Nat. Commun.*, 2021, **12**, 2870.
13. Y. Wang, A. Xu, Z. Wang, L. Huang, J. Li, F. Li, J. Wicks, M. Luo, D. H. Nam, C. S. Tan, Y. Ding, J. Wu, Y. Lum, C. T. Dinh, D. Sinton, G. Zheng and E. H. Sargent, *J. Am. Chem. Soc.*, 2020, **142**, 5702-5708.